Saikosaponin A protects against uremic toxin indole-3 acetic acid-induced damage to the myocardium

CHENG CHEN[1*], XIAOYUAN HU[2*] and XINGUANG CHEN[3]

[1]Department of Medical Science, Yangzhou Polytechnic College, Yangzhou, Jiangsu 225127; [2]Department of General Surgery, The First Affiliated Hospital of Soochow University, Soochow University, Suzhou, Jiangsu 215006; [3]Section of Pacing and Electrophysiology, Division of Cardiology, The First Affiliated Hospital of Gannan Medical University, Ganzhou, Jiangxi 341000, P.R. China

Received January 17, 2023; Accepted May 17, 2023

DOI: 10.3892/mmr.2023.13046

Abstract. Chronic kidney disease (CKD)-associated cardiac injury is a common complication in patients with CKD. Indole-3 acetic acid (IAA) is a uremic toxin that injures the cardiovascular system. Saikosaponin A (SSA) protects against pressure overload-induced cardiac fibrosis. However, the role and molecular mechanisms of IAA and SSA in CKD-associated cardiac injury remain unclear. The present study investigated the effects of IAA and SSA on CKD-associated cardiac injury in neonatal mouse cardiomyocytes and a mouse model of CKD. The expression of tripartite motif-containing protein 16 (Trim16), receptor interacting protein kinase 2 (RIP2) and phosphorylated-p38 were assessed using western blotting. The ubiquitination of RIP2 was measured by coimmunoprecipitation, and mouse cardiac structure and function were evaluated using hematoxylin and eosin staining and echocardiography. The results demonstrated that, SSA inhibited IAA-induced cardiomyocyte hypertrophy, upregulated Trim16 expression, downregulated RIP2 expression and decreased p38 phosphorylation. Furthermore, Trim16 mediated SSA-induced degradation of RIP2 by ubiquitination. In a mouse model of IAA-induced CKD-associated cardiac injury, SSA upregulated the protein expression levels of Trim16 and downregulated those of RIP2. Moreover, SSA alleviated heart hypertrophy and diastolic dysfunction in IAA-treated mice. Taken together, these results suggest that SSA is a protective agent against IAA-induced CKD-associated cardiac injury and that Trim16-mediated ubiquitination-related degradation of RIP2 and p38 phosphorylation may contribute to the development of CKD-associated cardiac injury.

Correspondence to: Dr Xinguang Chen, Section of Pacing and Electrophysiology, Division of Cardiology, The First Affiliated Hospital of Gannan Medical University, 128 Jinling West Road, Ganzhou, Jiangxi 341000, P.R. China
E-mail: chenxinguang.gy@gmu.edu.cn

[*]Contributed equally

Key words: saikosaponin A, indole-3 acetic acid, chronic kidney disease, cardiac injury

Introduction

Chronic kidney disease (CKD) affects millions of individuals globally (1). Mortality due to cardiovascular complications in patients with CKD is markedly higher than that in matched individuals from the general population (2). Cardiovascular disease (CVD) is the leading cause of death among CKD patients (3). In addition to accelerated atherosclerotic and vascular calcification, CKD-associated cardiac injury is also a vital cardiovascular complication of CKD, which is characterized by left ventricular hypertrophy (LVH) and diastolic dysfunction (4). Growing evidence suggests that uremic toxins serve an important role in the development of CKD-associated cardiac injury (5-8).

Indole-3 acetic acid (IAA) is a protein-bound uremic solute from tryptophan metabolism (9). The serum level of IAA is increased in patients with CKD compared with healthy individuals (10). In patients with uremia, IAA cannot be effectively removed by conventional dialysis and causes side effects, such as cardiovascular toxicity (11). Mortality and cardiovascular events are related to higher serum IAA in CKD patients; thus, IAA has been reported to predict these outcomes in CKD patients (10). However, the toxic effects of IAA on the heart and the underlying mechanisms of action remain unclear.

Saikosaponin A (SSA) is a triterpenoid saponin isolated from *Bupleuri radix*, a traditional medicinal herb with numerous bioactive agents (12). It has been reported to have certain pharmacological activities, such as anti-inflammatory and antioxidant effects (13). A previous study reported that SSA reduces pressure overload-induced myocardial fibrosis (14), indicating that SSA has a protective effect on the heart. Moreover, SSA inhibits lead-induced kidney injury (15).

Tripartite motif-containing protein 16 (Trim16), a member of the Trim family, has E3 ubiquitin ligase activity and serves an important role in certain diseases, such as pathological cardiac hypertrophy (16) and breast cancer (17). Receptor interacting protein kinase 2 (RIP2) belongs to the tyrosine kinase-like family (18). RIP2 overexpression aggravates myocardial infarction-related cardiac remodeling (19). Nevertheless,

whether SSA can help protect against CKD-associated cardiac injury, an important uremic cardiovascular complication, is still unknown. The present study investigated the protective effect of SSA against cardiac damage induced by IAA and explored the underlying mechanism and the roles of Trim16 and RIP2 in this process.

Materials and methods

Reagents and antibodies. DMEM, fetal bovine serum (FBS), trypsin and collagenase II were purchased from Gibco (Thermo Fisher Scientific, Inc.). Bromodeoxyuridine (BrdU) was purchased from Sigma-Aldrich (Merck KGaA, cat. no. 19-160). Rabbit anti-Trim 16 antibodies (cat. no. ab72129) and rabbit troponin antibodies (cat. no. ab209813) were purchased from Abcam. Rabbit anti-total p38 (t-p38) antibodies (cat. no. 8690), anti-phosphorylated p38 (p-p38) antibodies (cat. no. 4511) and K48-linked ubiquitin rabbit antibodies (cat. no. 4289) were purchased from Cell Signaling Technology, Inc. Rabbit anti-RIP 2 antibodies were purchased from Wuhan Sanying Biotechnology (cat. no. 15366-1-AP). Anti-tubulin antibodies (cat. no. 80762-1-RR) and anti-GAPDH antibodies (cat. no. 60004-1-Ig) were purchased from Wuhan Sanying Biotechnology. SSA and IAA were purchased from Med Chem Express (cat. no. HY-N0246) and Sigma-Aldrich (Merck KGaA; cat. no. 6505-45-9), respectively. Co-immunoprecipitation experiments were performed using a Pierce Co-Immunoprecipitation Kit (Thermo Fisher Scientific, Inc.; cat. no. 26149). PCR primers were purchased from Nanjing Ruizhen Biotechnology Co., Ltd. Trim16-specific and nonspecific small interfering RNAs (siRNAs) were purchased from Shanghai GenePharma Co., Ltd. Primary cell siRNA transfection reagent was purchased from Baidai Biology (cat. no. 11016).

Primary culture of neonatal cardiomyocytes from mice. Primary cardiomyocytes were isolated from neonatal mice 24-72 h post-birth obtained from the Animal Center of Gannan Medical College, as previously described (20). The left ventricular tissue was cut into small pieces (1 mm^3) using scissors and digested with digestion buffer (0.08% trypsin and 0.06% collagenase II dissolved in Hanks' Balanced Salt Solution) at 37˚C. After terminating digestion with complete DMEM (containing 10% FBS), the cardiomyocytes were cultured in DMEM with 10% FBS and 0.1 mM BrdU for 48 h. Cell culture medium was then replaced with complete DMEM (containing 10% FBS). Cardiomyocytes were identified via immunofluorescence with troponin. Briefly, cardiomyocytes were fixed in 4% paraformaldehyde for 10 min at room temperature and were washed five times with PBS for 10 min. After incubation with 0.2% Triton X-100 (Jiangsu KeyGEN BioTECH Corp., Ltd.) and blocking with 1% bovine serum albumin (Jiangsu KeyGEN BioTECH Corp., Ltd.) at room temperature, cardiomyocytes were incubated with anti-troponin antibodies (1:200; cat. no. ab209813; Abcam) overnight at 4˚C. The samples were then washed three times with PBS, followed by incubation with fluorescein isothiocyanate (FITC)-conjugated secondary antibodies (1:1,000; cat. no. ab7086; Abcam) at room temperature for 1 h. To visualize the nuclei of the cells, the cells were counterstained with 4,6-diamidino-2-phenylindole (DAPI) for 15 min at 37˚C. Images were captured with a fluorescence microscope system (Zeiss GmbH).

Animal treatment. Male C57BL/6J mice (n=24; age, 8 weeks; weight, 23-25 g) were bred from the Animal Center of Gannan Medical College. All mice were housed in the animal facility of Gannan Medical College at 19-21˚C under a 12 h light/dark cycle with free access to food and water. Eight-week-old mice were randomly assigned to the following experimental groups: Control (n=8), IAA-treated (n=8) (2.4 mg/kg/24 h IAA by oral gavage for 16 weeks) and IAA + SSA-treated (n=8) (2.4 mg/kg/24 h IAA by oral gavage and 40 mg/kg/24 h SSA through intraperitoneal injection for 16 weeks).

The mice were sacrificed at 16 weeks after the beginning of treatment by cervical dislocation after anesthetization with intraperitoneal injection of pentobarbital (50 mg/kg). For analysis, the heart of each animal was harvested.

Reverse transcription-quantitative PCR (RT-qPCR) analysis. Total RNA was extracted from the mouse cardiomyocytes and whole hearts using Trizol (Takara Bio, Inc.). The cDNA was prepared from 1 μg total RNA using the SuperScript First-Strand Synthesis system for RT-PCR (Invitrogen; Thermo Fisher Scientific, Inc.). qPCR was performed on a 10-μl reaction mixture containing 1 μl cDNA, 0.2 μl forward primer, 0.2 μl reverse primer, 3.8 μl distilled water and 4.8 μl EX Taq (Takara Bio, Inc.) using a real-time PCR detection system (Roche Diagnostics GmbH). The PCR program was as follows: Pre-denaturation at 94˚C for 1 min; followed by 30 cycles of denaturation at 94˚C for 30 sec, annealing at 60˚C for 30 sec and extension at 72˚C for 1 min. A final extension step was performed at 72˚C for 3 min. The relative expression of atrial natriuretic peptide (ANP), brain natriuretic peptide (BNP) and β-myosin heavy chain (β-MHC) mRNA was analyzed using the $2^{-\Delta\Delta Cq}$ method (21) and normalized to GAPDH. Based on the level of the control group, the results are presented as the fold increase. The primers used for qPCR were as follows: ANP forward (F), 5'-GGAGGAGAA GATGCCGGTAGA-3' and reverse (R), 5'-GCTTCCTCA GTCTGCTCACTCA-3'; BNP F, 5'-AAGCTGCTGGAGCTG ATAAGA-3' and R, 5'-GTTACAGCCCAAACGACTGAC-3'; β-MHC F, 5'-GTGCCAAGGGCCTGAATGAG-3' and R, 5'-GCAAAGGCTCCAGGTCTGA-3'; and GAPDH F, 5'-CCA AGGTCATCCATGACAACT-3' and R, 5'-GGGCCATCC ACAGTCTTCT-3'.

siRNA transfection. A Trim16-specific siRNA (siTrim16) and a nonspecific siRNA (siCntl) were purchased from GenePharma (Shanghai GenePharma Co., Ltd.). According to manufacturer's instructions 100 nmol/l siRNAs were transfected into cardiomyocytes with Primary Cell siRNA Transfection Reagent (cat. no. 11016; Baidai Biology) at room temperature. Briefly, cells ($5x10^6$ cells/ml) were seeded into six-well plates. siRNA (100 nM) was diluted in 400 μl serum-free culture medium, and 4 μl Primary Cell siRNA Transfection Reagent was added to it. Cells were incubated with the transfection complexes for 20 min at room temperature before being mixed with 1.6 ml fresh serum-free culture medium. After 8 h, the medium was replaced by fresh culture medium containing 10% FBS. Subsequently, cardiomyocytes

were treated with IAA (50 μmol/l) or SSA (30 μmol/l) for 48 h and used for assessment. The siRNA sequences used were as follows: TRIM16 sense, 5'-AGUAAUUCACCAUGC AGGUUU-3' and antisense, 5'-UCUCCCUCCUGCAUUUGU GUU-3'; and control (siCntl) sense, 5'-UUCUCAGAACGU GUCACGUTT-3' and antisense, 5'-ACGUGACAAGUUCGG AGAATT-3'.

Immunoblotting. Total protein was extracted from neonatal left ventricular heart sample tissues and cardiomyocytes using RIPA buffer (cat. no. KGP10100; Jiangsu KeyGEN BioTECH Corp., Ltd.). The protein concentration was detected using the BCA protein quantitative kit (cat. no. P0012; Beyotime Institute of Biotechnology). Protein (20 μg/lane) was separated by SDS-PAGE on 10% gels and was transferred to PVDF membranes (cat. no. FFP32; Beyotime Institute of Biotechnology). The membranes were blocked with 5% skimmed milk at room temperature for 30 min and incubated with primary antibodies against Trim16 (1:1,000; cat. no. ab72129; Abcam), t-p38 (1:1,000; cat. no. 8690; Cell Signaling Technology, Inc.), p-p38 (1:1,000; cat. no. 4511; Cell Signaling Technology, Inc.) and RIP2 (1:1,000; cat. no. 15366-1-AP; Wuhan Sanying Biotechnology) at 4˚C overnight. The membrane was then incubated with goat anti-rabbit secondary antibodies (1:5,000; cat. no. ZB2301; OriGene Technologies, Inc.). The intensity of the bands was assessed using a chemiluminescence kit (cat. no. 32209; Thermo Fisher Scientific, Inc.) and ImageJ software (version 1.5.3; National Institutes of Health).

Coimmunoprecipitation experiments. Coimmunoprecipitation experiments were performed utilizing a coimmunoprecipitation kit (cat. no. 26149; Thermo Fisher Scientific, Inc.). Total proteins from the cardiomyocytes were isolated using RIPA lysis buffer, and quantified using the BCA kit. For immunoprecipitation, 500 μg protein was incubated with 2 μg appropriate antibodies, including RIP2 antibodies (cat. no. 15366-1-AP; Wuhan Sanying Biotechnology) or IgG negative control antibodies (Beyotime Institute of Biotechnology; no. A7016) overnight at 4˚C. Subsequently, 40 μl Protein G/A agarose beads (Invitrogen; Thermo Fisher Scientific, Inc.) were added to the cell lysate and incubated for 2 h at room temperature. After beads were washed with PBS three times, precipitated proteins eluted from the beads (1 μg/μl) were resuspended in SDS-PAGE loading buffer, and boiled for 5 min. Finally, western blot analysis was used to measure the immunoprecipitation products as aforementioned.

Hematoxylin and eosin (H&E) staining. The hearts from mice were fixed in 10% paraformaldehyde for 48 h at room temperature. H&E staining was performed according to routine protocols. Briefly, for H&E staining, the heart slices were fixed using a graded alcohol series (100, 95, 85 and 70%) for 5 min and hydrated by immersion in 1% hydrochloric acid alcohol for 30 sec at room temperature. The slices were then stained using hematoxylin for 5 min and rinsed in water for 1 min at room temperature. The slices were subsequently stained with 0.5% eosin for 3 min. Finally, sections were covered using a coverslip and imaged under a light microscope (Zeiss GmbH).

Echocardiography and Doppler analysis. Echocardiography was performed using a high-resolution ultrasound imaging system (Vevo 2100, VisualSonics, Inc.) to assess cardiac structure and function. The mouse was fixed in the supine position and anesthetized through inhalation of 2% isoflurane/100% oxygen. Left ventricular end-diastolic anterior wall depth (LVAWd), left ventricular end-systolic anterior wall depth (LVAWs), left ventricular end-diastolic posterior wall depth (LVPWd), left ventricular end-systolic posterior wall depth (LVPWs) and left ventricular diastolic function indicators, such as the ratio of left ventricular transmitral early peak flow velocity to left ventricular transmitral late peak flow velocity (E/A ratio) (22), were recorded.

Serum biochemistry analysis. The mice were anesthetized via an intraperitoneal injection of pentobarbital (50 mg/kg) and were sacrificed by exsanguination performed after removal of the eyeball. Blood collected from the retro-orbital vein was centrifuged at 157 x g for 5 min at 4˚C, and the serum was collected and stored at -80˚C. Serum creatinine (Cr) and blood urea nitrogen (BUN) levels were measured by Roche automatic biochemical analysis. Levels of BUN and Cr were evaluated by urease-glutamate dehydrogenase and enzymatic methods, respectively. BUN assay kits (cat. no. OSR6234) and Cr assay kits (batch no. 20220912) were provided by Beckman Coulter, Inc. and Shanghai KHB Co., Ltd., respectively.

Statistical analysis. SPSS statistical software (version 20.0, IMB Corp.) was used for data analysis. The differences between groups were determined by one-way analysis of variance (ANOVA) and Tukey's post hoc test was used following ANOVA. Values are presented as the mean ± standard deviation and $P<0.05$ was considered to indicate a statistically significant difference.

Results

SSA alleviates cardiomyocyte hypertrophy induced by IAA. Cultured mouse cardiomyocytes were treated with various concentrations of IAA. Compared with the control group, the mRNA expression levels of ANP, BNP and β-MHC in the 10 and 50 μmol/l IAA-treated groups were significantly increased (Fig. 1A). Furthermore, SSA treatment inhibited cardiomyocyte hypertrophy induced by IAA. Compared with those in the 50 μmol/l IAA group, the mRNA expression levels of ANP, BNP and β-MHC in the 30 μmol/l SSA-treated groups were significantly decreased (Fig. 1B).

SSA inhibits downregulation of Trim16 expression and upregulation of RIP2 expression induced by IAA. Cardiomyocytes were transfected with (siCntl) or siTrim16. Compared with the untransfected control and siCntl groups, the protein expression level of Trim16 in the siTrim16 group was significantly decreased (Fig. 2A). Cardiomyocytes were treated with either IAA (50 μmol/l) or IAA + SSA (50 μmol/l IAA + 30 μmol/l SSA). Compared with the control group, the protein expression level of Trim16 in the IAA-only group was significantly decreased, and SSA treatment significantly blocked this decrease (Fig. 2B). Cardiomyocytes were treated with siCntl, IAA (50 μmol/l IAA + siCntl), IAA + SSA (50 μmol/l

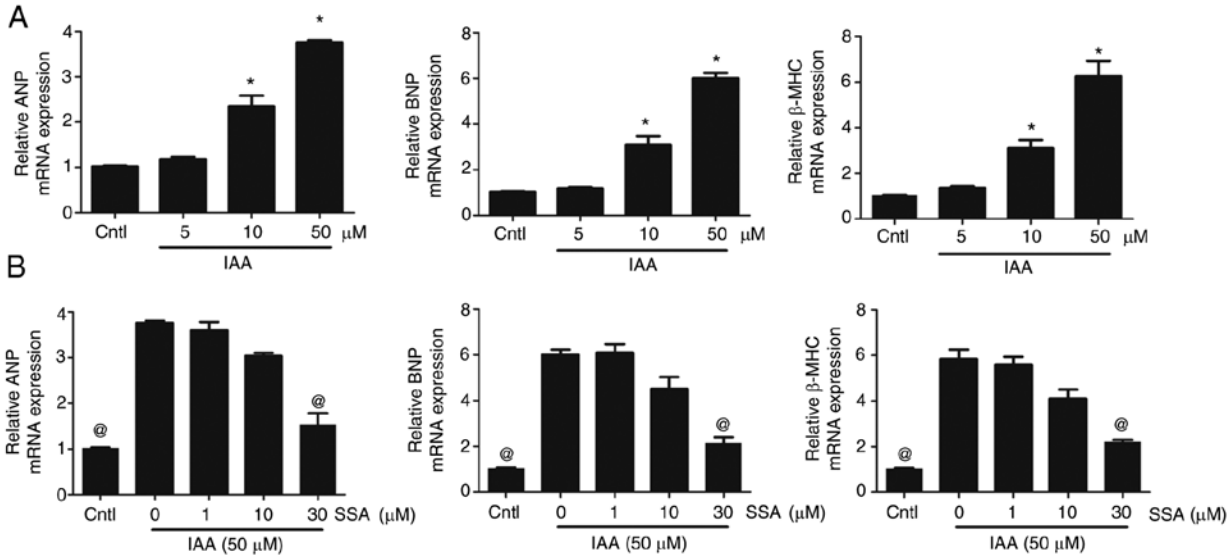

Figure 1. SSA inhibits IAA-induced cardiomyocyte hypertrophy. (A) Cardiomyocytes were treated with different concentrations of IAA (5, 10 and 50 μmol/l) for 48 h and mRNA expression levels of ANP, BNP and β-MHC were analyzed by qPCR. (B) Cardiomyocytes were pretreated with SSA (1, 10 and 30 μmol/l) for 1 h then exposed to IAA (50 μmol/l) for 48 h and mRNA expression levels of ANP, BNP and β-MHC were analyzed by qPCR. *P<0.01 vs. Cntl, $^{@}$P<0.01 vs. 50 μmol/l IAA group. SSA, saikosaponin A; IAA, indole-3 acetic acid; ANP, atrial natriuretic peptide; BNP, brain natriuretic peptide; β-MHC, β-myosin heavy chain; Cntl, control; qPCR, quantitative PCR.

IAA + 30 μmol/l SSA + siCntl) or IAA + SSA + siTrim16 (50 μmol/l IAA + 30 μmol/l SSA + siTrim16). Compared with the control siCntl group, the protein expression level of RIP2 in the IAA-treated group was significantly upregulated, but SSA treatment significantly inhibited this IAA-induced RIP2 upregulation. Notably, Trim16 knockdown significantly blocked the inhibitory effect of SSA on RIP2 upregulation (Fig. 2C).

SSA alleviates cardiomyocyte hypertrophy induced by IAA and silencing of Trim16 blocks the anti-hypertrophic effect of SSA. Cardiomyocytes were treated with siCntl, IAA (50 μmol/l IAA + siCntl), IAA + SSA (50 μmol/l IAA + 30 μmol/l SSA + siCntl) or and IAA + SSA + siTrim16 (50 μmol/l IAA + 30 μmol/l SSA + siTrim16). Compared with the control group, the mRNA expression levels of ANP, BNP and β-MHC in the IAA-treated group were significantly increased. The mRNA expression levels of ANP, BNP and β-MHC in the IAA + SSA-treated group were significantly downregulated compared with that in the IAA-only group. Trim16 knockdown significantly reduced the inhibitory effect of SSA on the expression of ANP, BNP and β-MHC (Fig. 3A). Immunofluorescence analysis of the morphological alterations in cardiomyocytes demonstrated that SSA inhibited cardiomyocyte hypertrophy induced by IAA. Silencing Trim16 blocked the antihypertrophic effect of SSA (Fig. 3B). The phosphorylation of p38 was significantly increased in the IAA-treated group compared with that in the control group, however, SSA treatment significantly decreased the phosphorylation of p38. Moreover, the effect of SSA was significantly blocked by silencing Trim16 (Fig. 3C).

IAA inhibits K48 ubiquitination of RIP2 in cardiomyocytes and SSA-induced RIP2 ubiquitination in a Trim16-dependent manner. Cardiomyocytes were treated with siCntl, IAA (50 μmol/l IAA + siCntl), IAA + SSA (50 μmol/l IAA +

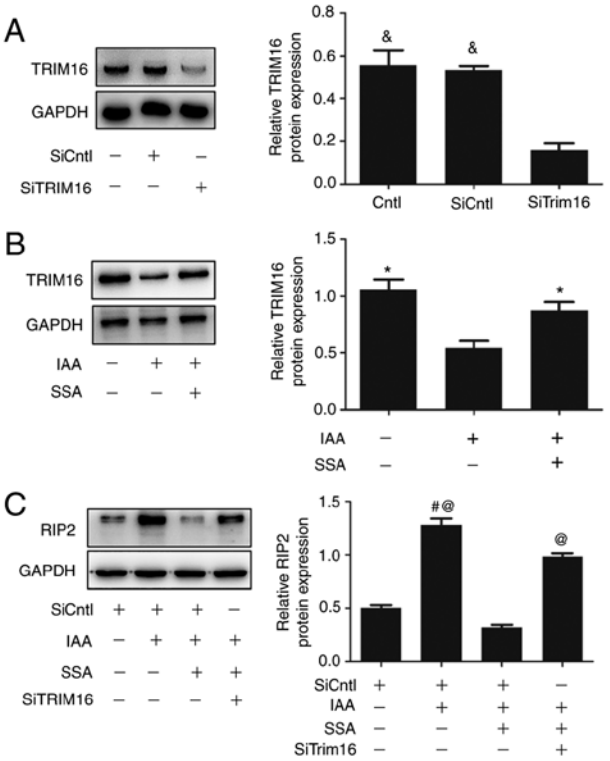

Figure 2. SSA inhibits Trim16 and RIP2 expression in IAA-treated cardiomyocytes. (A) SiTrim16 or scrambled siRNA (siCntl) were transfected into cardiomyocytes and Trim16 protein expression determined by western blotting. (B) Cardiomyocytes were pretreated with SSA (30 μmol/l) for 1 h and then exposed to IAA (50 μmol/l) for 48 h and Trim16 protein expression measured by Western blotting. (C) SiTrim16 or scrambled siRNA (siCntl) was transfected into cardiomyocytes. Cardiomyocytes were pretreated with 30 μmol/l SSA for 1 h and incubated with IAA (50 μmol/l) for 48 h. RIP2 protein expression was determined by western blotting. *P<0.05 vs. IAA-treated group, $^{\&}$P<0.01 vs. siTrim16 group, $^{\#}$P<0.01 vs. siCntl group, $^{@}$P<0.01 vs. IAA + SSA-treated group. SSA, saikosaponin A; IAA, indole-3 acetic acid; Trim16, tripartite motif-containing protein 16; RIP2, receptor interacting protein kinase 2.

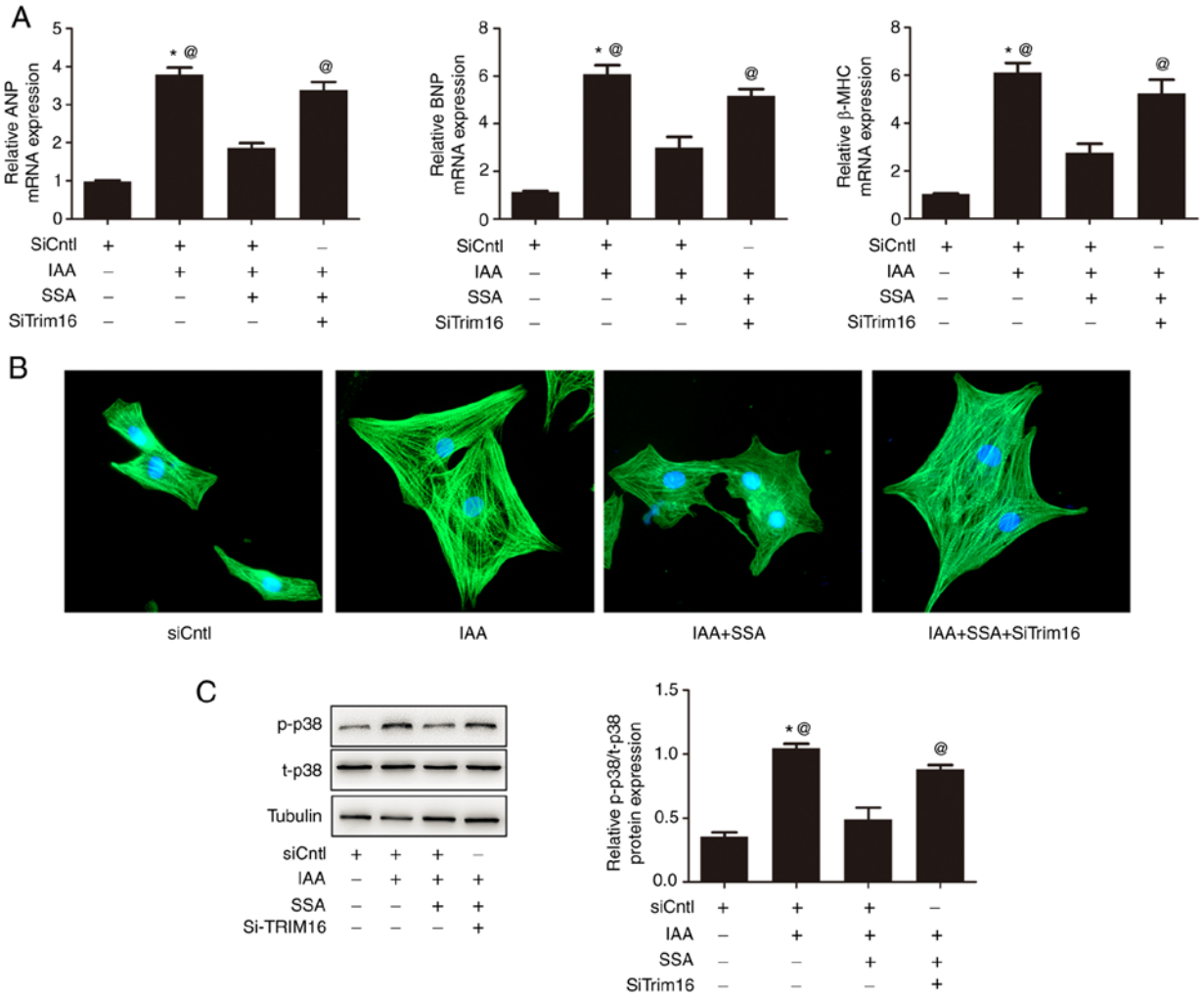

Figure 3. Silencing of Trim16 blocks the inhibitory effect of SSA on cardiomyocyte hypertrophy induced by IAA. Cardiomyocytes were transfected with siTrim16 or scrambled siRNA (siCntl), treated with SSA (30 μmol/l) for 1 h then treated with IAA (50 μmol/l) for 48 h. (A) mRNA expression of ANP, BNP and β-MHC were measured by quantitative PCR. (B) Cell size was observed by immunofluorescence using a troponin antibody (magnification, x400). (C) Expression of p-p38 and t-p38 was measured by western blotting. *P<0.01 vs. siCntl, $^{@}$P<0.01 vs. IAA + SSA-treated group. SSA, saikosaponin A; IAA, indole-3 acetic acid; Trim16, tripartite motif-containing protein 16; ANP, atrial natriuretic peptide; BNP, brain natriuretic peptide; β-MHC, β-myosin heavy chain; p, phosphorylated; t, total.

30 μmol/l SSA + siCntl) or IAA + SSA + siTrim16 (50 μmol/l IAA + 30 μmol/l SSA + siTrim16). Compared with the control group, K48 ubiquitination of RIP2 in cardiomyocytes in the IAA-treated group was significantly decreased. SSA significantly increased the K48 ubiquitination of RIP2. Furthermore, this effect of SSA was significantly reduced by silencing Trim16 (Fig. 4).

SSA alleviates structural and functional abnormalities of the heart induced by IAA in mice. Male C57BL/6J mice were divided into control, IAA-treated and IAA + SSA-treated groups. Compared with those in the control group, the levels of BUN and Cr in the IAA-treated group were significantly increased 16 weeks after IAA administration. Treatment of mice with SSA did not decrease the IAA-mediated increase in BUN and Cr levels (Fig. 5A). Compared with the control group, mRNA expression levels of ANP, BNP and β-MHC in the heart were significantly increased in the IAA-treated group (Fig. 5B). Administration of SSA significantly reduced the expression of ANP, BNP and β-MHC (Fig. 5B). In addition, an increase in cardiac hypertrophy in IAA-treated mice compared with that in the control group was observed using H&E staining. Treatment with SSA alleviated the cardiac hypertrophy observed in IAA-treated mice (Fig. 5C).

Echocardiography demonstrated that the LVPWs, LVPWd, LVAWs and LVAWd in the IAA-treated group of mice were significantly higher than those in the control group (Fig. 6A). Treatment with SSA significantly decreased the LVPWs, LVPWd, LVAWs and LVAWd in IAA-treated mice (Fig. 6A). Analysis of the Doppler-derived mitral flow velocities demonstrated that there was a significant reduction in the E/A ratio in the IAA-treated mice. Such an alteration is always accompanied by diastolic relaxation abnormalities (10), which indicated that IAA treatment impaired cardiac diastolic function. However, SSA treatment significantly ameliorated cardiac diastolic function in IAA-treated mice (Fig. 6B).

Effect of IAA and SSA on the expression of Trim16, RIP2 and p38 in mice. Compared with the control group, the expression of Trim16 in the heart in the IAA-treated mice was significantly

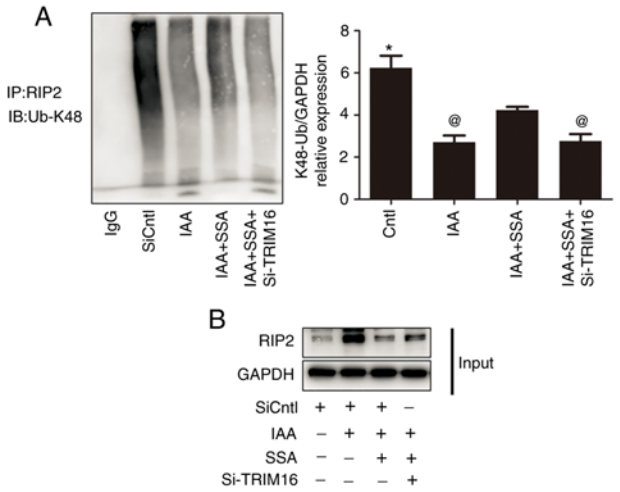

Figure 4. SSA alleviates the inhibitory effect of IAA on the K48 ubiquitination of RIP2 in cardiomyocytes. (A) Cardiomyocytes were transfected with siTrim16 or scrambled siRNA (siCntl), treated with SSA (30 μmol/l) for 1 h, then incubated with IAA (50 μmol/l) for 48 h. K48 ubiquitination of RIP2 was measured by immunoprecipitation. (B) Expression of RIP2 was measured by western blotting *P<0.01 vs. IAA-treated group, $^{@}$P<0.05 vs. IAA + SSA-treated group. SSA, saikosaponin A; IAA, indole-3 acetic acid; RIP2, receptor interacting protein kinase 2; p, phosphorylated; t, total; IP, immunoprecipitation; IB, immunoblotting; si, short interfering RNA.

decreased; however, the expression of RIP2 and phosphorylation of p38 in the IAA-treated group were significantly increased. Intraperitoneal injection of SSA significantly inhibited the downregulation of Trim16 expression, significantly upregulated RIP2 expression and significantly increased phosphorylation of p38 in the heart of IAA-treated mice (Fig. 6C).

Discussion

CKD is a global health issue which has attracted much attention (23). It is estimated that 10-14% of the global population have CKD (4). Patel *et al* (4) reported a total of 37 and 2.6 million patients with CKD in the USA and UK, respectively. As CKD progresses, certain complications can occur, among which cardiovascular complications are particularly important (24-26). CKD-associated cardiac injury (also known as uremic cardiomyopathy) is a widely prevalent cardiovascular disease in patients with CKD, which accounts for ~50% of deaths due to CKD (27). CKD-associated cardiac injury leads to left ventricular hypertrophy, left ventricular dilation and left ventricular diastolic dysfunction. Severe CKD-associated cardiac injury can lead to sudden cardiac death even in individuals without cardiac symptoms (28).

Although previous studies have reported that hypertension, volume overload, insulin resistance and hyperphosphatemia serve important roles in CKD-associated cardiac injury, the drivers and molecular mechanisms underlying CKD-associated cardiac injury are still unclear. Since 2015, mounting evidence (7,29) has indicated that uremic toxins have a vital role in the development of CKD-associated cardiac injury.

The uremic toxin indoxyl sulfate (IS) induces cardiomyocyte hypertrophy *in vitro* and *in vivo* (6,30). Moreover, our previous study reported that another uremic toxin, p-cresyl sulfate (PCS), also induced cardiomyocyte hypertrophy (5). In addition to IS and PCS, IAA is another important uremic toxin (7,10). IAA is a protein-bound uremic toxin that is mainly produced during tryptophan metabolism by intestinal bacteria (31). Liabeuf *et al* (31) reported that serum IAA progressively increased with CKD stage. Claro *et al* (32) demonstrated a negative correlation between eGFR and IAA in patients with CKD in pre-dialysis. Dou *et al* (10) reported that mortality and the occurrence of cardiovascular events were significantly higher in individuals with serum IAA levels >3.73 mmol/l compared with serum IAA levels <3.73 mmol/l in a study that followed 120 patients with CKD over 966 days. Multivariate Cox regression analysis has been reported to demonstrate that serum IAA level can predict cardiovascular events and mortality after adjusting for age, sex, cholesterol, systolic blood pressure, smoking, C-reactive protein, serum phosphorus, body mass index, albumin, diastolic blood pressure and history of cardiovascular disease (10). Notably, when IS, PCS and IAA were integrated into a multivariate Cox regression model, only IAA predicted cardiovascular events and mortality, which suggests that there was a close association between high serum IAA and cardiovascular complications in CKD (10). Chinnappa *et al* (33) reported that IAA was closely associated with peak cardiac power and aerobic exercise capacity in patients with CKD.

Stockler-Pinto *et al* (34) reported that IAA stimulated production of nuclear factor-kappa B (NF-κB) mRNA and decreased nuclear E2-related factor 2 (Nrf2) expression in hemodialysis patients, which indicated that IAA triggered inflammation and oxidative stress in these individuals. Bataille *et al* (35) reported that there was no apparent association of IAA with anemia parameters in hemodialysis patients. Therefore, further in-depth studies on the role of IAA in complications of CKD should be performed. Furthermore, IAA activates the aryl hydrocarbon receptor (AhR)/p38MAPK/NF-κB signaling pathway and upregulates the expression of the proinflammatory enzyme cyclooxygenase-2 in endothelial cells *in vitro* (10). IAA treatment also increases production of reactive oxygen species in endothelial cells (10). Addi *et al* (36) reported that IAA induced tissue factor expression in multiple types of endothelial cells, such as human umbilical vein endothelial cells (HUVECs), aortic endothelial cells and cardiac-derived microvascular cells. NF-κB p50 subunit translocation induced by IAA serves a key role in this process (36). Furthermore, inhibition of the AhR/p38MAPK signaling pathway reduces tissue factor expression upregulation in IAA-treated endothelial cells (36). Previous clinical and basic studies demonstrate that IAA has a damaging effect on the cardiovascular system, however, few studies on IAA in CKD-associated cardiac injury have been previously reported. Recently, Hager *et al* (37) reported that IAA prompted cardiac necrosis in rats. The present study demonstrated that IAA upregulated the expression of ANP, BNP and β-MHC in mouse cardiomyocytes and induced cardiomyocyte hypertrophy *in vitro*. Moreover, cardiac hypertrophy, decreased diastolic function and increased expression of ANP, BNP and β-MHC were demonstrated to occur in mice treated with IAA. Therefore, IAA could induce CKD-associated cardiac injury both *in vivo* and *in vitro*.

SSA is a triterpenoid saponin isolated from *R. bupleuri* (12) that exerts numerous pharmacological effects involving

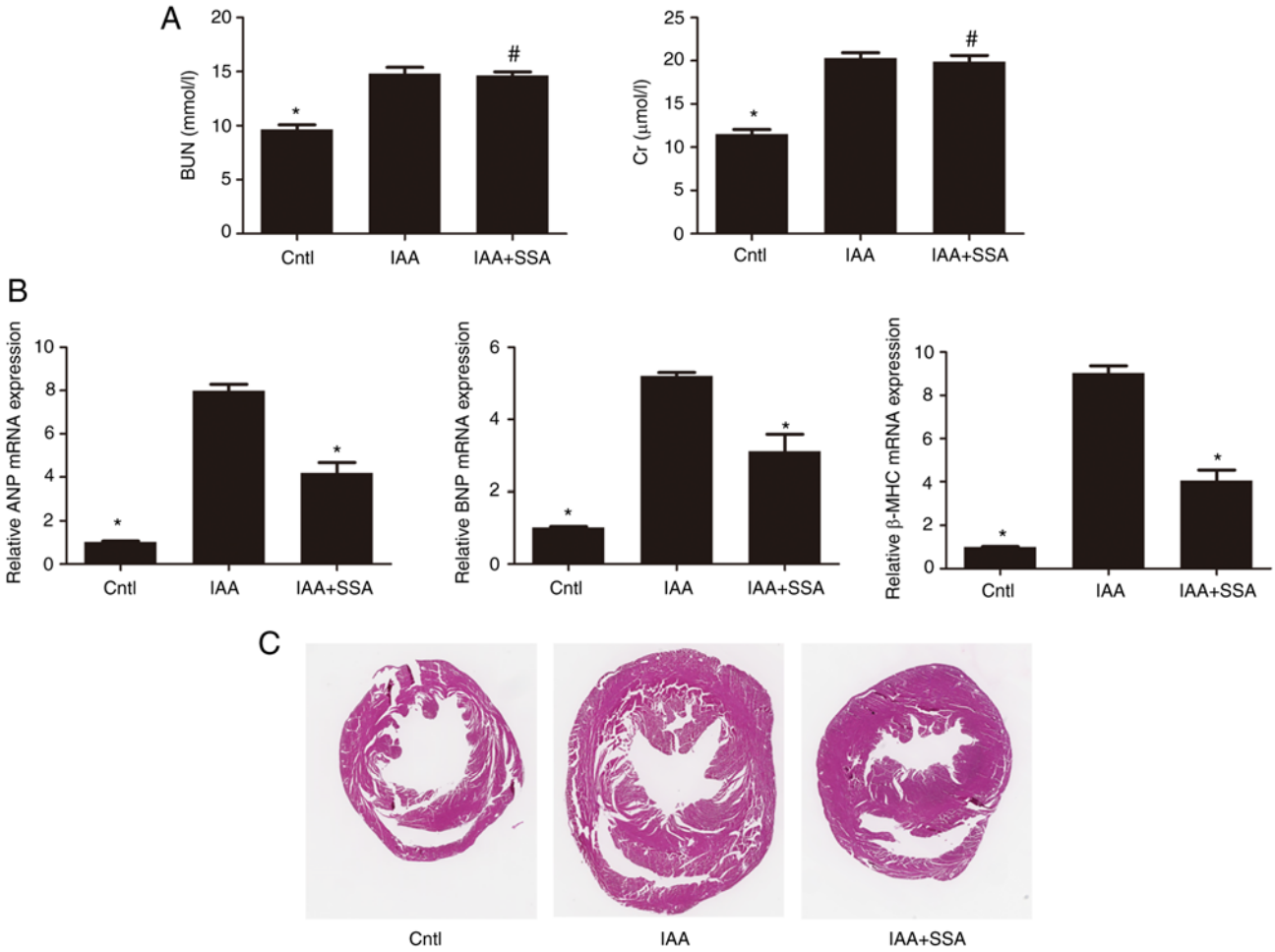

Figure 5. SSA treatment ameliorates IAA-induced cardiac hypertrophy in mice. (A) Serum BUN and Cr levels in the control (n=8), IAA (n=8) and IAA + SSA (n=8) groups of mice were analyzed by urease-glutamate dehydrogenase and enzymatic methods, respectively. (B) The mRNA expression of ANP, BNP and β-MHC in the myocardial tissues of control, IAA- IAA + SSA-treated groups of mice were analyzed by quantitative PCR. (C) Representative micrographs (magnification, 10x) of hematoxylin and eosin-stained transverse sections from hearts of control, IAA- and IAA + SSA-treated mice. *P<0.01 vs. IAA-treated group; #P<0.01 vs. Cntl. SSA, Saikosaponin A; IAA, Indole-3 acetic acid; ANP, Atrial natriuretic peptide; BNP, Brain natriuretic peptide; β-MHC, β-myosin heavy chain; Cntl, control; BUN, blood urea nitrogen; Cr, serum creatinine.

antioxidative stress and anti-inflammation (13). SSA regulates the expression of bone morphogenetic protein 4 in hepatic stellate cells (38). SSA also attenuates liver inflammation and fibrosis induced by carbon tetrachloride (39). Zhou *et al* (40) reported that SSA alleviated ulcerative colitis through an anti-inflammatory pathway. Du *et al* (41) reported that SSA alleviated lipopolysaccharide (LPS)-induced acute lung injury in mice by reducing the expression of TNF-α and IL-1β. Furthermore, SSA demonstrates protective effects against neuronal damage induced by ischemia-reperfusion injury, and this mechanism involves downregulation of Toll-like receptor 4 and NF-κB expression in the brain (42). There are few reports of the effect of SSA on cardiovascular disease. Fu *et al* (43) reported that SSA inhibited LPS-induced oxidative stress and inflammation in HUVECs. He *et al* (44) reported that SSA attenuated atherosclerosis by inhibiting the PI3K/Akt/NF-κB/NLRP3 signaling pathway. A previous study reported that SSA alleviated pressure overload-induced cardiac fibrosis (14). Zhang *et al* (45) reported that Saikosaponin D, another similar triterpenoid saponin isolated from *R. bupleuri*, efficiently protected cardiomyocytes from Doxorubicin-induced cardiotoxicity by inhibiting excessive oxidative stress. In addition, SSA has a protective effect on the kidney (15) and complications of chronic kidney disease (46). Huang *et al* demonstrated that SSA improved CKD-induced muscle atrophy by reducing oxidative stress through the PI3K/AKT/Nrf2 pathway (46). However, there has been little research on whether SSA alleviates CKD-associated cardiac injury. In the present study, administration of SSA inhibited cardiomyocyte hypertrophy induced by IAA. This confirmed that SSA reduced ANP, BNP and β-MHC expression in cardiomyocytes and reduced the size of these cells, reversing the increased expression and size of cells induced by IAA treatment.

Trim16, a member of the Trim family of proteins (47), was first identified as an estrogen-responsive B-box protein which possesses transcriptional activity (48). The molecular structure of Trim16 is different from other members of the Trim family, as it lacks the RING finger domain (RING domain) (49). Trim16 has numerous functions, including regulation of cell differentiation, the innate immune response and tumorigenesis (50-53). The majority of Trim family members have E3 ubiquitin ligase activity and serve an important role in protein posttranslational modification (47). Although Trim16 lacks the

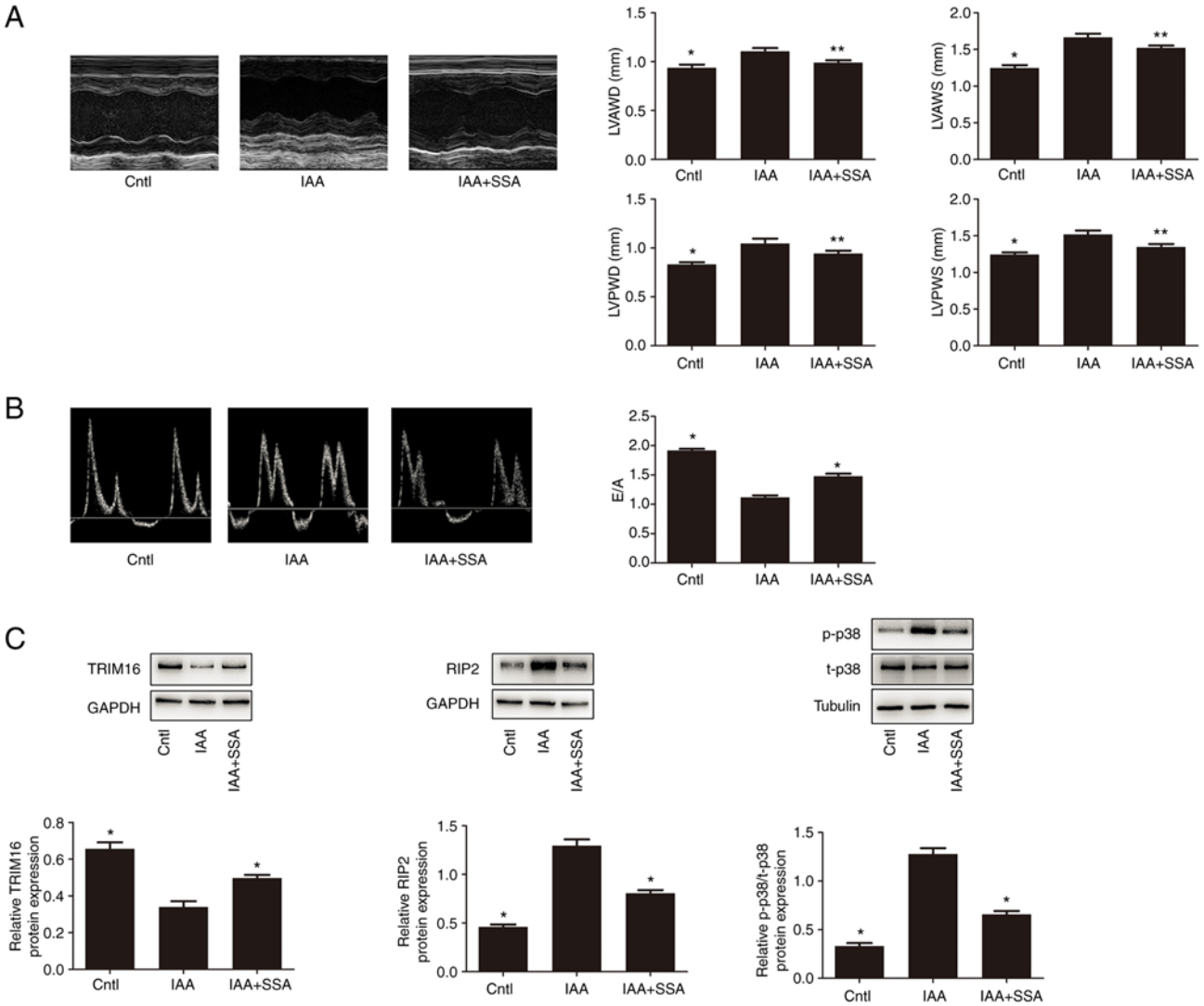

Figure 6. SSA treatment ameliorates structural and functional abnormalities of the heart in echocardiography of mice treated with IAA, and also regulates expression of Trim16, RIP2 and p-p38 in the heart. (A) Representative M-mode echocardiograms and the mean LVPWs, LVPWd, LVAWs and LVAWd in the control, IAA- and IAA + SSA-treated groups. (B) Representative M-mode echocardiograms and the mean E/A in the control, IAA- and IAA + SSA-treated groups. (C) Expression of Trim16, RIP2, p-p38 and t-p38 measured by western blotting. *P<0.01, **P<0.05 vs. IAA-treated group. SSA, saikosaponin A; IAA, indole-3 acetic acid; Trim16, tripartite motif-containing protein 16; p, phosphorylated; Cntl, control; RIP2, receptor interacting protein kinase 2; LVPWd, left ventricular end-diastolic posterior wall depth; LVPWs, left ventricular end-systolic posterior wall depth; LVAWd, left ventricular end-diastolic anterior wall depth; LVAWs, left ventricular end-systolic anterior wall depth.

RING domain, it has two B-box domains and has E3 ubiquitin ligase activity.

Certain Trim family proteins, such as Trim8, Trim24, Trim32 and Trim72, have been reported to serve key roles in cardiac hypertrophy and other cardiovascular diseases, which indicated that the TRIM family serve a critical role in heart disease (54,55). Although the role of the Trim family in cardiac development, cardiomyopathy and other cardiac diseases has been widely reported, the role of Trim16 in cardiac diseases is still unclear. Trim16 inhibits inflammation and oxidative stress, which are often closely associated with cardiovascular disease (56,57). A previous study (16) found that Trim16 deficiency aggravated phenylephrine-induced cardiomyocyte hypertrophy *in vitro* and transverse aortic constriction-induced mouse cardiac hypertrophy *in vivo*, whereas overexpression of Trim16 inhibited cardiac hypertrophy. The underlying mechanism was reported to be Trim16-increased ubiquitination of Scr kinase (16). However, the role of Trim16 in CKD-associated cardiac injury is currently unknown. In the present study, the expression of Trim16 was downregulated in hypertrophic cardiomyocytes treated with IAA, and SSA alleviated cardiomyocyte hypertrophy and upregulated Trim16 expression, which suggested that Trim16 may be involved in CKD-associated cardiac injury.

RIP2 belongs to the tyrosine kinase-like family of proteins (18). RIP2 is involved in the transduction of multiple signaling pathways, such as the IKK/NF-κB and MAPK/AP1 signaling pathways (18) , which implied that RIP2 may serve an important role in the occurrence and development of certain diseases, such as myocardial ischemia and septic cardiomyopathy (58,59). RIP2 overexpression aggravates myocardial infarction-related cardiac remodeling, and its mechanism is related to the activation of p38 phosphorylation (19). Previously (60), it was demonstrated that the expression of RIP2 was significantly increased in cardiac cells in patients with heart failure, mice with aortic banding

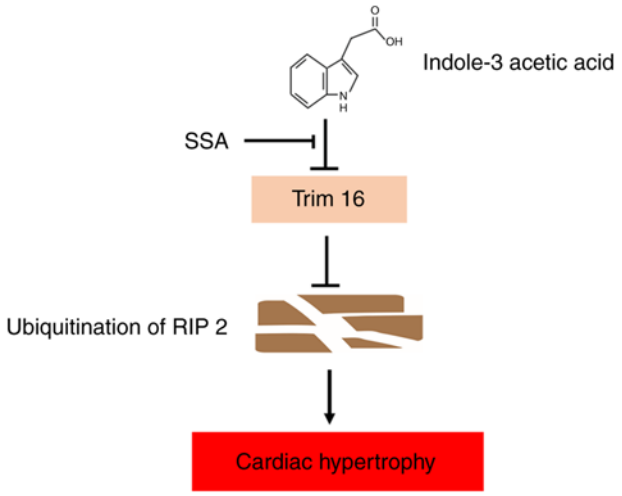

Figure 7. Schematic representation of the IAA-induced damage in cardiomyocytes. IAA downregulates the expression of Trim16, which resulted in decreased K48 ubiquitination of RIP2 and increased expression of RIP2. Increased RIP2 expression induces cardiomyocyte hypertrophy and damages diastolic dysfunction of the heart. SSA protects cardiomyocytes from the effects of IAA by upregulating Trim16. SSA, saikosaponin A; IAA, indole-3 acetic acid; Trim16, tripartite motif-containing protein 16; RIP2, receptor interacting protein kinase 2.

surgery-induced pressure overload and phenylephrine-treated cardiomyocytes *in vitro*. Notably, RIP2 overexpression aggravates pressure overload-induced cardiac remodeling (60). The expression and function of RIP2 in CKD-associated cardiac injury have not yet been confirmed. The present study demonstrated that the expression of RIP2 and phosphorylated p38 was upregulated in hypertrophic cardiomyocytes treated with IAA. Furthermore, SSA inhibited the upregulation of RIP2 expression and p38 phosphorylation. Humphries *et al* reported that RIP2 can be modified by ubiquitination, which in turn affects the signaling pathway function of RIP2 (18). Trim16 has E3 ubiquitin ligase activity and RIP2 can be regulated by ubiquitination (49,61), however, whether Trim16 can regulate RIP2 ubiquitination has not been previously reported. The present study demonstrated that upregulation of Trim16 promoted RIP2 K48 ubiquitination, which is normally associated with protein degradation, which indicated that Trim16 alleviated CKD-associated cardiac injury by increasing the ubiquitination of RIP2 at K48 and promoting RIP2 degradation. Moreover, the present study demonstrated that Trim16 knockdown blocked the inhibitory effect of SSA on IAA-induced upregulation of RIP2 expression and cardiomyocyte hypertrophy.

In the present study, an IAA-induced CKD-associated cardiac injury mouse model was established. Mice were administered IAA by oral gavage for 16 weeks and echocardiography analysis demonstrated increased LVAWd, LVAWs, LVPWs and LVPWd in IAA-treated mice. In addition, heart hypertrophy was also observed in IAA-treated mice. Analysis of the Doppler-derived mitral flow velocity demonstrated a reduction in the diastolic function of the heart in IAA-treated mice. Administration of SSA improved cardiac hypertrophy and diastolic dysfunction. Moreover, SSA inhibited IAA-induced downregulation of TRIM16 expression, upregulation of RIP2 expression and p38 phosphorylation in the hearts of CKD-associated cardiac injury mice.

The present study had certain limitations. First, the conclusions were not tested in transgenic mouse models. If the toxicity of IAA is reduced in TRIM16-overexpressing and RIP2-knockout mice, the evidence to support this mechanism would be stronger. In addition, IAA impairs renal function, so the damaging effect of IAA on the heart may be related to the deterioration of renal function. If the concentration of other uremic toxins such as IS and PCS in the serum of mice were measured, more rigorous results would be obtained.

In summary, the present study demonstrated that the uremic toxin IAA induced cardiomyocyte hypertrophy via regulation of RIP2 ubiquitination mediated by TRIM16 and p38 phosphorylation and that SSA antagonized the damaging effects of IAA (Fig. 7). The present study provided novel information on the posttranslational modification of RIP2 by IAA and SSA. As a result of these findings, new insights into CKD-associated cardiac injury have been reported and have the potential to contribute to the future development of treatments for this disease.

Acknowledgements

Not applicable.

Funding

The present study was funded by the Green Yang golden phoenix plan of Yangzhou (grant no. YZLYJFJH2021YXBS027), The Science and Technology Plan Project of Jiangxi Province Health and Health Commission (grant no. 202210913) and The Guiding Science and Technology Plan Project of Ganzhou (grant no. GZ2021ZSF105).

Availability of data and materials

The datasets used and/or analyzed during the current study are available from the corresponding author on reasonable request.

Authors' contributions

CC and XC conceived and designed the experiments. XC and XH performed the experiments. CC analyzed the data and wrote the original draft. XC reviewed and edited the manuscript. CC and XC confirm the authenticity of all the raw data. All authors read and approved the final manuscript.

Ethics approval and consent to participate

All animal protocols were approved by the Animal Ethical and Welfare Committee of Gannan Medical College (approval no. 2021092).

Patient consent for publication

Not applicable.

Authors' information

XC ORCID ID: 0000-0002-9206-4145

Competing interests

The authors declare that they have no competing interests.

References

1. Lv JC and Zhang LX: Prevalence and disease burden of chronic kidney disease. Adv Exp Med Biol 1165: 3-15, 2019.
2. Webster AC, Nagler EV, Morton RL and Masson P: Chronic kidney disease. Lancet 389: 1238-1252, 2017.
3. Matsushita K, Ballew SH, Wang AY, Kalyesubula R, Schaeffner E and Agarwal R: Epidemiology and risk of cardiovascular disease in populations with chronic kidney disease. Nat Rev Nephrol 18: 696-707, 2022.
4. Patel N, Yaqoob MM and Aksentijevic D: Cardiac metabolic remodelling in chronic kidney disease. Nat Rev Nephrol 18: 524-537, 2022.
5. Chen C, Xie C, Xiong Y, Wu H, Wu L, Zhu J, Xing C and Mao H: Damage of uremic myocardium by p-cresyl sulfate and the ameliorative effect of Klotho by regulating SIRT6 ubiquitination. Toxicol Lett 367: 19-31, 2022.
6. Yang K, Wang C, Nie L, Zhao X, Gu J, Guan X, Wang S, Xiao T, Xu X, He T, *et al*: Klotho protects against indoxyl sulphate-induced myocardial hypertrophy. J Am Soc Nephrol 26: 2434-2446, 2015.
7. Han H, Zhu J, Zhu Z, Ni J, Du R, Dai Y, Chen Y, Wu Z, Lu L and Zhang R: p-Cresyl sulfate aggravates cardiac dysfunction associated with chronic kidney disease by enhancing apoptosis of cardiomyocytes. J Am Heart Assoc 4: e001852, 2015.
8. Wu CC, Hsieh MY, Hung SC, Kuo KL, Tsai TH, Lai CL, Chen JW, Lin SJ, Huang PH and Tarng DC: Serum indoxyl sulfate associates with postangioplasty thrombosis of dialysis grafts. J Am Soc Nephrol 27: 1254-1264, 2016.
9. Jourde-Chiche N, Dou L, Cerini C, Dignat-George F, Vanholder R and Brunet P: Protein-bound toxins-update 2009. Semin Dial 22: 334-339, 2009.
10. Dou L, Sallée M, Cerini C, Poitevin S, Gondouin B, Jourde-Chiche N, Fallague K, Brunet P, Calaf R, Dussol B, *et al*: The cardiovascular effect of the uremic solute indole-3 acetic acid. J Am Soc Nephrol 26: 876-887, 2015.
11. Shi Y, Tian H, Wang Y, Shen Y, Zhu Q and Ding F: Improved dialysis removal of protein-bound uraemic toxins with a combined displacement and adsorption technique. Blood Purif 51: 548-558, 2022.
12. Shuai-Cheng W, Xiu-Ling C, Jian-Qing S, Zong-Mei W, Zhen-Jiang Y and Lian-Tao L: Saikosaponin A protects chickens against pullorum disease via modulation of cholesterol. Poult Sci 98: 3539-3547, 2019.
13. Zhu Y, Chen X, Rao X, Zheng C and Peng X: Saikosaponin a ameliorates l ipopolysaccharide and d-galactosamine-induced liver injury via activating LXRα. Int Immunopharmacol 72: 131-137, 2019.
14. Liu Y, Gao L, Zhao X, Guo S, Liu Y, Li R, Liang C, Li L, Dong J, Li L and Yang H: Saikosaponin a protects from pressure overload-induced cardiac fibrosis via inhibiting fibroblast activation or endothelial cell endMT. Int J Biol Sci 14: 1923-1934, 2018.
15. Song Y, Sun H, Gao S, Tang K, Zhao Y, Xie G and Gao H: Saikosaponin a attenuates lead-induced kidney injury through activating Nrf2 signaling pathway. Comp Biochem Physiol C Toxicol Pharmacol 242: 108945, 2021.
16. Liu J, Li W, Deng KQ, Tian S, Liu H, Shi H, Fang Q, Liu Z, Chen Z, Tian T, *et al*: The E3 ligase TRIM16 is a key suppressor of pathological cardiac hypertrophy. Circ Res 130: 1586-1600, 2022.
17. Roshanazadeh MR, Adelipour M, Sanaei A, Chenane H and Rashidi M: TRIM3 and TRIM16 as potential tumor suppressors in breast cancer patients. BMC Res Notes 15: 312, 2022.
18. Humphries F, Yang S, Wang B and Moynagh PN: RIP kinases: Key decision makers in cell death and innate immunity. Cell Death Differ 22: 225-236, 2015.
19. Jacquet S, Nishino Y, Kumphune S, Sicard P, Clark JE, Kobayashi KS, Flavell RA, Eickhoff J, Cotton M and Marber MS: The role of RIP2 in p38 MAPK activation in the stressed heart. J Biol Chem 283: 11964-1171, 2008.
20. Ravi V, Jain A, Taneja A, Chatterjee K and Sundaresan NR: Isolation and culture of neonatal murine primary cardiomyocytes. Curr Protoc 1: e196, 2021.
21. Livak KJ and Schmittgen TD: Analysis of relative gene expression data using real-time quantitative PCR and the 2(-Delta Delta C(T)) method. Methods 25: 402-408, 2001.
22. Oh JK, Appleton CP, Hatle LK, Nishimura RA, Seward JB and Tajik AJ: The noninvasive assessment of left ventricular diastolic function with two-dimensional and Doppler echocardiography. J Am Soc Echocardiogr 10: 246-270, 1997.
23. Glassock RJ, Warnock DG and Delanaye P: The global burden of chronic kidney disease: Estimates, variability and pitfalls. Nat Rev Nephrol 13: 104-114, 2017.
24. Chen TK, Knicely DH and Grams ME: Chronic kidney disease diagnosis and management: A review. JAMA 322: 1294-1304, 2019.
25. Thomas R, Kanso A and Sedor JR: Chronic kidney disease and its complications. Prim Care 35: 329-344, 2008.
26. House AA, Wanner C, Sarnak MJ, Piña IL, McIntyre CW, Komenda P, Kasiske BL, Deswal A, deFilippi CR, Cleland JGF, *et al*: Heart failure in chronic kidney disease: Conclusions from a kidney disease: Improving global outcomes (KDIGO) controversies conference. Kidney Int 95: 1304-1317, 2019.
27. Chen C, Xie C, Wu H, Wu L, Zhu J, Mao H and Xing C: Uraemic cardiomyopathy in different mouse models. Front Med (Lausanne) 8: 690517, 2021.
28. Cao XS, Chen J, Zou JZ, Zhong YH, Teng J, Ji J, Chen ZW, Liu ZH, Shen B, Nie YX, *et al*: Association of indoxyl sulfate with heart failure among patients on hemodialysis. Clin J Am Soc Nephrol 10: 111-119, 2015.
29. Yamaguchi K, Yisireyili M, Goto S, Cheng XW, Nakayama T, Matsushita T, Niwa T, Murohara T and Takeshita K: Indoxyl sulfate activates NLRP3 inflammasome to induce cardiac contractile dysfunction accompanied by myocardial fibrosis and hypertrophy. Cardiovasc Toxicol 22: 365-377, 2022.
30. Fernandez-Prado R, Esteras R, Perez-Gomez MV, Gracia-Iguacel C, Gonzalez-Parra E, Sanz AB, Ortiz A and Sanchez-Niño MD: Nutrients turned into toxins: Microbiota modulation of nutrient properties in chronic kidney disease. Nutrients 9: 489, 2017.
31. Liabeuf S, Laville SM, Glorieux G, Cheddani L, Brazier F, Beauport DT, Valholder R, Choukroun G and Massy ZA: Difference in profiles of the gut-derived tryptophan metabolite indole acetic acid between transplanted and non-transplanted patients with chronic kidney disease. Int J Mol Sci 21: 2031, 2020.
32. Claro LM, Moreno-Amaral AN, Gadotti AC, Dolenga CJ, Nakao LS, Azevedo MLV, de Noronha L, Olandoski M, de Moraes TP, Stinghen AEM and Pécoits-Filho R: The impact of uremic toxicity induced inflammatory response on the cardiovascular burden in chronic kidney disease. Toxins (Basel) 10: 384, 2018.
33. Chinnappa S, Tu YK, Yeh YC, Glorieux G, Vanholder R and Mooney A: Association between protein-bound uremic toxins and asymptomatic cardiac dysfunction in patients with chronic kidney disease. Toxins (Basel) 10: 520, 2018.
34. Stockler-Pinto MB, Soulage CO, Borges NA, Cardozo LFM, Dolenga CJ, Nakao LS, Pecoits-Filho R, Fouque D and Mafra D: From bench to the hemodialysis clinic: Protein-bound uremic toxins modulate NF-κB/Nrf2 expression. Int Urol Nephrol 50: 347-354, 2018.
35. Bataille S, Pelletier M, Sallée M, Berland Y, McKay N, Duval A, Gentile S, Mouelhi Y, Brunet P and Burtey S: Indole 3-acetic acid, indoxyl sulfate and paracresyl-sulfate do not influence anemia parameters in hemodialysis patients. BMC Nephrol 18: 251, 2017.
36. Addi T, Poitevin S, McKay N, El Mecherfi KE, Kheroua O, Jourde-Chiche N, de Macedo A, Gondouin B, Cerini C, Brunet P, *et al*: Mechanisms of tissue factor induction by the uremic toxin indole-3 acetic acid through aryl hydrocarbon receptor/nuclear factor-kappa B signaling pathway in human endothelial cells. Arch Toxicol 93: 121-136, 2019.
37. Hager THI: Assessment toxic effects of exposure to 3-indoleacetic acid via hemato-biochemical, hormonal, and histopathological screening in rats. Environ Sci Pollut Res Int 29: 90703-90718, 2022.
38. Wang X, Wang Q, Burczynski FJ, Kong W and Gong Y: Saikosaponin A of Bupleurum chinense (Chaihu) elevates bone morphogenetic protein 4 (BMP-4) during hepatic stellate cell activation. Phytomedicine 20: 1330-1335, 2013.
39. Wu SJ, Tam KW, Tsai YH, Chang CC and Chao JC: Curcumin and saikosaponin a inhibit chemical-induced liver inflammation and fibrosis in rats. Am J Chin Med 38: 99-111, 2010.
40. Zhou F, Wang N, Yang L, Zhang LC, Meng LJ and Xia YC: Saikosaponin A protects against dextran sulfate sodium-induced colitis in mice. Int Immunopharmacol 72: 454-458, 2019.

41. Du ZA, Sun MN and Hu ZS: Saikosaponin a Ameliorates LPS-induced acute lung injury in mice. Inflammation 41: 193-198, 2018.
42. Wang X and Yang G: Saikosaponin A attenuates neural injury caused by ischemia/reperfusion. Transl Neurosci 11: 227-235, 2020.
43. Fu Y, Hu X, Cao Y, Zhang Z and Zhang N: Saikosaponin a inhibits lipopolysaccharide-oxidative stress and inflammation in Human umbilical vein endothelial cells via preventing TLR4 translocation into lipid rafts. Free Radic Biol Med 89: 777-785, 2015.
44. He D, Wang H, Xu L, Wang X, Peng K, Wang L, Liu P and Qu P: Saikosaponin-a attenuates oxidized LDL uptake and prompts cholesterol efflux in THP-1 cells. J Cardiovasc Pharmacol 67: 510-518, 2016.
45. Zhang YJ, Wu SS, Chen XM, Pi JK, Cheng YF, Zhang Y, Wang XJ, Luo D, Zhou JH, Xu JY, *et al*: Saikosaponin D alleviates DOX-induced cardiac injury in vivo and in vitro. J Cardiovasc Pharmacol 79: 558-567, 2022.
46. Huang M, Yan Y, Deng Z, Zhou L, She M, Yang Y, Zhang M and Wang D: Saikosaponin A and D attenuate skeletal muscle atrophy in chronic kidney disease by reducing oxidative stress through activation of PI3K/AKT/Nrf2 pathway. Phytomedicine 114: 154766, 2023.
47. Ozato K, Shin DM, Chang TH and Morse HC III: TRIM family proteins and their emerging roles in innate immunity. Nat Rev Immunol 8: 849-860,2008.
48. Spirina LV, Yunusova NV, Kondakova IV and Tarasenko NV: Transcription factors Brn-3α and TRIM16 in cancers, association with hormone reception. Heliyon 5: e02090, 2019.
49. Bell JL, Malyukova A, Holien JK, Koach J, Parker MW, Kavallaris M, Marshall GM and Cheung BB: TRIM16 acts as an E3 ubiquitin ligase and can Heterodimerize with other TRIM family members. PLoS One 7: e37470, 2012.
50. Jena KK, Mehto S, Kolapalli SP, Nath P, Sahu R, Chauhan NR, Sahoo PK, Dhar K, Das SK, Chauhan S and Chauhan S: TRIM16 governs the biogenesis and disposal of stress-induced protein aggregates to evade cytotoxicity: Implication for neurodegeneration and cancer. Autophagy 15: 924-926, 2019.
51. Kim PY, Tan O, Liu B, Trahair T, Liu T, Haber M, Norris MD, Marshall GM and Cheung BB: High TDP43 expression is required for TRIM16-induced inhibition of cancer cell growth and correlated with good prognosis of neuroblastoma and breast cancer patients. Cancer Lett 374: 315-323, 2016.
52. Chauhan S, Kumar S, Jain A, Ponpuak M, Mudd MH, Kimura T, Choi SW, Peters R, Mandell M, Bruun JA, *et al*: TRIMs and galectins globally cooperate and TRIM16 and galectin-3 co-direct autophagy in endomembrane damage homeostasis. Dev Cell 39: 13-27, 2016.
53. Di Rienzo M, Romagnoli A, Antonioli M, Piacentini M and Fimia GM: TRIM proteins in autophagy: Selective sensors in cell damage and innate immune responses. Cell Death Differ 27: 887-902, 2020.
54. Borlepawar A, Rangrez AY, Bernt A, Christen L, Sossalla S, Frank D and Frey N: TRIM24 protein promotes and TRIM32 protein inhibits cardiomyocyte hypertrophy via regulation of dysbindin protein levels. J Biol Chem 292: 10180-10196, 2017.
55. Chen L, Huang J, Ji Y, Zhang X, Wang P, Deng K, Jiang X, Ma G and Li H: Tripartite motif 32 prevents pathological cardiac hypertrophy. Clin Sci 130: 813-828, 2016.
56. Zhao Y, Liu H, Xi X, Chen S and Liu D: TRIM16 protects human periodontal ligament stem cells from oxidative stress-induced damage via activation of PICOT. Exp Cell Res 397: 112336, 2020.
57. Jena KK, Kolapalli SP, Mehto S, Nath P, Das B, Sahoo PK, Ahad A, Syed GH, Raghav SK, Senapati S, *et al*: TRIM16 controls assembly and degradation of protein aggregates by modulating the p62-NRF2 axis and autophagy. EMBO J 37: e98358, 2018.
58. Andersson L, Täng MS, Lundqvist A, Lindbom M, Mardani I, Fogelstrand P, Shahrouki P, Redfors B, Omerovic E, Levin M, *et al*: Rip2 modifies VEGF-induced signalling and vascular permeability in myocardial ischaemia. Cardiovasc Res 107: 478-486, 2015.
59. Lin Z, Liao HH, Zhou ZY, Zhang N, Li WJ and Tang QZ: RIP2 inhibition alleviates lipopolysaccharide-induced septic cardiomyopathy via regulating TAK1 signaling. Eur J Pharmacol 947: 175679, 2023.
60. Yang JJ, Zhang N, Zhou ZY, Ni J, Feng H, Li WJ, Mou SQ, Wu HM, Deng W, Liao HH and Tang QZ: Cardiomyocyte-specific RIP2 overexpression exacerbated pathologic remodeling and contributed to spontaneous cardiac hypertrophy. Front Cell Dev Biol 9: 688238, 2021.
61. Yang S, Wang B, Humphries F, Jackson R, Healy ME, Bergin R, Aviello G, Hall B, McNamara D, Darby T, *et al*: Pellino3 ubiquitinates RIP2 and mediates Nod2-induced signaling and protective effects in colitis. Nat Immunol 14: 927-936, 2013.